Contribution from the Department of Chemistry,
State University of New York at Buffalo, Buffalo, New York 14214

Crystal Structure and Molecular Geometry of Dimeric Azulenemanganese Tricarbonyl, $[(C_{10}H_8)Mn(CO)_3]_2$

MELVYN ROWEN CHURCHILL,* ROMANA A. LASHEWYCZ, and FRANK J. ROTELLA

Received July 26, 1976 AIC60537V

The complex $[(C_{10}H_8)Mn(CO)_3]_2$, previously prepared from $H_3Mn_3(CO)_{12}$ and azulene, has been characterized via a complete three-dimensional x-ray diffraction study. The complex crystallizes in the centrosymmetric monoclinic space group $P2_1/c$ with a = 14.482 (1) Å, b = 10.416 (2) Å, c = 14.896 (2) Å, β = 93.56 (1)°, V = 2242.6 (5) Å^3, ρ(obsd) = 1.580 (10) g cm^{-3}, and ρ(calcd) = 1.582 g cm^{-3} for mol wt 534.29 and Z = 4. Diffraction data were collected with a Syntex $P2_1$ automated diffractometer using graphite-monochromatized Mo Kα radiation. The structure was solved by symbolic addition and refined by difference-Fourier and least-squares techniques. All atoms, including hydrogen atoms, have been located and refined; final discrepancy indices are R_F = 3.98% and R_{wF} = 3.17% for all 2946 symmetry-independent reflections in the range $4° < 2\theta \leq 45°$. The molecule contains a 4,4′-diazulene ligand in which each of the two five-membered rings is bonded to a $Mn(CO)_3$ group via a π-cyclopentadienyl→metal linkage. The molecule may be named systematically as hexacarbonyl(1,2,3,9,10-η^5;1′,2′,3′,9′,10′-η^5-4,4′-diazulene)dimanganese. The individual $[(C_{10}H_8)Mn(CO)_3]_2$ molecules are each chiral (the absolute configurations at the 4 and 4′ positions being identical); however, the crystal contains an ordered racemic array by virtue of the $\bar{1}$ and c-glide operations of space group $P2_1/c$. Bond distances within the halves of the molecule are in excellent agreement, ranges being Mn–CO = 1.781 (3)–1.800 (3) Å, Mn–C(azulene) = 2.127 (3)–2.191 (2) Å, C–O = 1.144 (4)–1.154 (3) Å, C–C(cyclopentadienyl) = 1.394 (4)–1.434 (3) Å, C(sp^2)–C(sp^3) = 1.495 (4)–1.505 (3) Å, C(sp^2)=C(sp^2) = 1.316 (4)–1.331 (4) Å, and C(sp^2)–C(sp^2) = 1.440 (4)–1.455 (4) Å; the C(sp^3)–C(sp^3) linkage between the two azulene moieties is 1.580 (3) Å.

Introduction

We have previously reported the results of extensive x-ray crystallographic studies on a variety of complexes of azulene (I) and substituted azulenes, including $(C_{10}H_8)Fe_2(CO)_5$,[1]

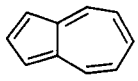

I

$(C_{10}H_8)Mo_2(CO)_6$,[2] $[(i\text{-}C_3H_7)(CH_3)_2C_{10}H_5]Mo_2(CO)_6$,[3] $[(C_{10}H_8)Mo(CO)_3CH_3]_2$,[4] $(C_{10}H_8)Mn_2(CO)_6$,[5] $(C_{10}H_8)_2Fe_4(CO)_{10}$,[6] $(C_{10}H_8)_2Fe$,[7] $[(CH_3)_3C_{10}H_5]Ru_4(CO)_9$,[8] and $(C_{10}H_8)Ru_3(CO)_7$.[9]

It has been noted previously[10] that, in our hands, the reaction of azulene with $Mn_2(CO)_{10}$ yielded only $(C_{10}H_8)Mn_2(CO)_6$[5] (II) whereas Burton, Pratt, and Wilkinson[11] reported that only

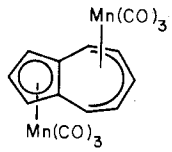

II

$[(C_{10}H_8)Mn(CO)_3]_2$ was obtained from this reaction. This discrepancy has been a source of irritation to us for some years.

Recently King and Ackermann[12] reported the synthesis of $[(C_{10}H_8)Mn(CO)_3]_2$ via a different route, i.e., from $H_3Mn_3(CO)_{12}$ and azulene. We have now undertaken a crystal structure analysis of $[(C_{10}H_8)Mn(CO)_3]_2$ obtained from this source. Our results are reported below.

Experimental Section

Yellow crystals of $[(C_{10}H_8)Mn(CO)_3]_2$ were supplied by Professor R. B. King of the University of Georgia. A needle-shaped crystal of length 0.2 mm and diameter 0.08 mm was selected for the structural analysis. It was mounted on the tip of a thin glass fiber which was then inserted into a 0.2-mm diameter Lindemann glass capillary. The capillary was flushed with nitrogen, flame-sealed, and seated into a brass pin on a eucentric goniometer using modeling clay and glue.

The goniometer was mounted on a Syntex $P2_1$ four-circle automated diffractometer under the control of a Nova 1200 computer.

Since this is the first structural study performed by this research group using this instrument, experimental techniques will be described in detail, the intention being to refer back to this description in future reports.

The diffractometer was equipped with a molybdenum x-ray tube [λ(Mo Kα_1) 0.709 300 Å, λ(Mo Kα_2) 0.713 590 Å, λ(Mo K$\bar{\alpha}$) 0.710 730 Å],[14] operated at 50 kV and 20 mA, and a highly oriented graphite monochromator mounted with equatorial geometry.[15]

The crystal was centered in a random orientation with the needle axis (later shown to be c) offset by about 15° from coincidence with the ϕ axis. Determination of the crystal orientation, unit cell parameters, and crystal quality was accomplished by the following procedure.

(1) A random-orientation rotation photograph was taken with $2\theta = \omega = \chi = 0°$ with the ϕ axis rotating at 234°/min for 20 min. The photograph was recorded on a flat Polaroid film cassette mounted 97.5 mm from the crystal.

(2) Film separations ($2x_i$, $2y_i$) of 15 quartets of reflections were converted into diffractometer coordinates for individual reflections (2θ and χ are directly calculable, ω is defined as 0°, and ϕ is determined by rotating the crystal until a peak of intensity greater than 10^3 counts/s is encountered) and were centered by an automatic routine.

(3) The three shortest independent reciprocal vectors obtained from (2) were used to generate, by linear combinations, real-space vectors as possible unit-cell axes. All combinations which produced integral (±0.1) values for the indices of all 15 reflections were printed out, along with the cosines of the angles between each pair of vectors. A monoclinic cell was then chosen by inspection.

(4) Axial photographs were taken about each of the three axes chosen in (3), using the Polaroid cassette attached to the diffractometer. The m symmetry about the b axis was confirmed and all three axes selected above were found, by inspection, to be true solutions (rather than submultiples of the true axial lengths).

(5) The 15 reflections were assigned indices consistent with the unit cell selected, via an autoindexing routine.

(6) All data in the angular range $30° < 2\theta \leq 35°$ were now collected at the maximum scan rate (29.3°/min). From these, 15 strong reflections, well dispersed in reciprocal space, were selected for least-squares refinement. Their 2θ, ω, and χ settings were determined via an automatic centering routine. These values were used in the least-squares refinement of cell parameters and orientation parameters. [Because of dispersion by the monochromator, the Kα_1 and Kα_2 components are not resolved. The wavelength of Mo K$\bar{\alpha}$ radiation was used in determining cell constants.]

(7) Both θ–2θ and ω scans were recorded graphically for selected reflections along each of the principal reciprocal axes, in order to check on the quality of the peak profiles and their spread in ω under standard operating conditions. All were found to be satisfactory.

(8) Several low-order reflections were measured at 10° intervals of ψ (the azimuthal angle corresponding to rotation of the crystal about its diffraction vector) from $\psi = 0°$ to $\psi = 350°$. The intensities thus

Table I. Data for the X-Ray Diffraction Study of $[(C_{10}H_8)Mn(CO)_3]_2$

(A) Crystal Data

Crystal system: monoclinic	$V = 2242.6$ (5) Å^3
Space group: $P2_1/c$ [C_{2h}^5; No. 14]	$T = 24$ °C
$a = 14.4820$ (11) Å	$Z = 4$
$b = 10.4160$ (18) Å	Mol wt 534.290
$c = 14.8958$ (19) Å	ρ(obsd)[a] = 1.580 (10) g cm^{-3}
$\beta = 93.555$ (9) °	ρ(calcd) = 1.582 g cm^{-3}

(B) Intensity Data

Radiation: Mo Kα
Monochromator: highly oriented graphite
Reflections measd: $+h, +k, \pm l$
Max 2θ: 45°
Min 2θ: 4°
Scan type: θ–2θ
Scan speed: 1.0°/min.
Scan range: symmetrical, $[2.0 + \Delta(\alpha_2 - \alpha_1)]$°
Reflections collected: 3492 total; 2946 independent
Max dev of std reflections: 400, 1.86%; 033, 1.33%; 322, 1.48%
Absorption coeff: 11.21 cm^{-1}; no absorption correction made (see text)

[a] Measured by neutral buoyancy in aqueous barium iodide.

obtained all showed variations of less than 5% with ψ, indicating that absorption corrections could safely be neglected.

Intensity data were now collected via a θ(crystal)–2θ(counter) scan in 96 steps using bisecting geometry. The scan was from [2θ(Mo Kα_1) − 1.0]° to [2θ(Mo Kα_2) + 1.0]°. Any step of the scan which exceeded 5000 counts was subjected to a linear correction for coincidence losses. [This correction is valid to about 50 000 counts/interval; no reflections greater than this magnitude were encountered during the structural study.] Backgrounds (B_1 and B_2) were measured both at the beginning and at the end of the scan, each for half the time of the scan. The stability of the entire assembly was monitored by measuring three strong check reflections after every 50 data. No significant changes were found. The net intensity (I) and its standard deviation ($\sigma(I)$) were calculated from

$$I = SC - \tau(B_1 + B_2)$$

$$\sigma(I) = [SC + \tau^2(B_1 + B_2) + p^2I^2]^{1/2}$$

where SC is the count during the scan, τ is the ratio of scan time to background time (=1 in the present study) and p (the ignorance factor) was set equal to 0.035. Any negative value for I was reset to zero. No reflections were rejected as "not significantly above background".

The unscaled structure factor amplitude $|F|$ is given by $|F| = (I/Lp)^{1/2}$. Its standard deviation, $\sigma(|F|)$, was calculated as $\sigma(|F|) = |F| - (|F|^2 - \sigma(I)/Lp)^{1/2}$ for $I \geq \sigma(I)$ and $\sigma(|F|) = (\sigma(I)/Lp)^{1/2}$ for $I < \sigma(I)$.

The Lp factor for a monochromator in the equatorial mode is given by

$$Lp = \frac{0.5}{\sin 2\theta}\left[\left(\frac{1 + (\cos^2 2\theta_M)(\cos^2 2\theta)}{1 + \cos^2 2\theta_M}\right) + \left(\frac{1 + |\cos 2\theta_M|\cos^2 2\theta}{1 + |\cos 2\theta_M|}\right)\right]$$

This equation assumes that the graphite monochromator crystal is 50% mosaic and 50% perfect. The monochromator angle, $2\theta_M$, is 12.2° for Mo Kα radiation.

An examination of the data set revealed the systematic absences $h0l$ for $l = 2n + 1$ and $0k0$ for $k = 2n + 1$, consistent with the space group $P2_1/c$. The systematically absent reflections were rejected.

Numerical information on data collection is given in Table I.

Solution and Refinement of the Structure

Programs used during the structural analysis include FAME (Wilson plot and generation of $|E|$ values, by R. B. K. Dewar and A. L. Stone), MAGIC (phase generation from $|E|$ values via symbolic addition, by Dewar and Stone), LINEX74 (structure factor calculations and full-matrix least-squares refinement, derived from ORFLS, by W. R. Busing, K. O. Martin, and H. A. Levy), JIMDAP (Fourier synthesis, derived from the program FORDAP by A. Zalkin), ORFFE (calculation of distances and angles with esd's, by Busing, Martin, and Levy), PLOD (least-squares planes, by B. G. DeBoer), and ORTEP (thermal ellipsoid plotting program, by C. K. Johnson). All calculations were performed

Table II. Statistics for Intensity Distribution in $[(C_{10}H_8)Mn(CO)_3]_2$

Quantity	Obsd	Theoretical[a] Centrosym	Theoretical[a] Non-centrosym
$\langle\|E\|^2\rangle$	1.000[b]	1.000	1.000
$\langle\|E\|\rangle$	0.799	0.798	0.886
$\langle\|E^2 - 1\|\rangle$	0.965	0.968	0.736
$\|E\| > 1.0$ (%)	31.61	32.0	37.0
$\|E\| > 2.0$ (%)	4.48	5.00	1.80
$\|E\| > 3.0$ (%)	0.14	0.3	0.01

[a] I. L. Karle, K. S. Dragonette, and S. A. Brenner, *Acta Crystallogr.*, 19, 713 (1965). [b] Fixed by an adjustable scale factor.

Table III. Final Positional Parameters, with Esd's,[a] for $[(C_{10}H_8)Mn(CO)_3]_2$

Atom	x	y	z
Mn(1)	0.749 096 (24)	0.307 985 (35)	0.170 420 (22)
Mn(2)	0.853 227 (23)	0.709 326 (34)	0.536 329 (23)
C(11)	0.814 66 (18)	0.298 16 (28)	0.073 35 (17)
O(11)	0.859 14 (14)	0.292 24 (25)	0.012 26 (13)
C(12)	0.658 99 (18)	0.397 52 (26)	0.110 04 (16)
O(12)	0.601 97 (14)	0.455 69 (20)	0.071 66 (13)
C(13)	0.692 94 (19)	0.156 36 (29)	0.147 45 (18)
O(13)	0.658 13 (17)	0.058 53 (21)	0.136 67 (16)
C(21)	0.886 86 (18)	0.609 61 (26)	0.629 89 (17)
O(21)	0.908 08 (16)	0.544 91 (21)	0.690 57 (14)
C(22)	0.754 01 (17)	0.759 59 (25)	0.594 26 (16)
O(22)	0.692 47 (13)	0.789 19 (20)	0.634 74 (13)
C(23)	0.923 40 (18)	0.840 02 (27)	0.580 29 (18)
O(23)	0.969 68 (15)	0.922 38 (21)	0.607 61 (15)
C(1A)	0.827 85 (19)	0.242 10 (28)	0.288 19 (17)
C(2A)	0.873 65 (18)	0.344 54 (30)	0.249 56 (17)
C(3A)	0.816 41 (17)	0.454 17 (26)	0.250 25 (15)
C(4A)	0.659 82 (15)	0.509 95 (23)	0.317 11 (15)
C(5A)	0.563 34 (17)	0.457 02 (26)	0.303 08 (16)
C(6A)	0.532 97 (19)	0.344 40 (29)	0.328 38 (18)
C(7A)	0.584 28 (21)	0.237 82 (28)	0.368 10 (18)
C(8A)	0.673 71 (21)	0.212 01 (25)	0.362 10 (17)
C(9A)	0.740 36 (16)	0.287 16 (22)	0.315 14 (14)
C(10A)	0.733 89 (15)	0.419 14 (21)	0.291 11 (13)
C(1B)	0.894 80 (19)	0.752 92 (30)	0.404 07 (17)
C(2B)	0.933 56 (18)	0.636 34 (29)	0.432 85 (18)
C(3B)	0.860 03 (18)	0.551 65 (25)	0.446 05 (17)
C(4B)	0.681 58 (16)	0.553 45 (23)	0.417 84 (15)
C(5B)	0.605 24 (17)	0.635 23 (28)	0.449 40 (17)
C(6B)	0.588 10 (19)	0.756 09 (31)	0.427 93 (21)
C(7B)	0.641 44 (22)	0.843 02 (29)	0.376 66 (21)
C(8B)	0.731 37 (22)	0.840 84 (26)	0.366 01 (19)
C(9B)	0.796 53 (16)	0.742 59 (23)	0.398 50 (15)
C(10B)	0.775 11 (15)	0.614 64 (21)	0.426 10 (14)
H(1A)	0.847 2 (16)	0.156 4 (23)	0.295 0 (15)
H(2A)	0.933 9 (17)	0.343 1 (23)	0.225 8 (16)
H(3A)	0.830 3 (15)	0.539 8 (23)	0.229 6 (15)
H(4A)	0.663 7 (12)	0.584 8 (19)	0.282 6 (12)
H(5A)	0.519 0 (14)	0.515 7 (21)	0.277 1 (14)
H(6A)	0.469 2 (17)	0.328 1 (23)	0.319 4 (15)
H(7A)	0.545 2 (17)	0.176 3 (25)	0.397 8 (17)
H(8A)	0.702 2 (15)	0.136 4 (24)	0.389 5 (15)
H(1B)	0.924 4 (18)	0.827 8 (26)	0.392 7 (17)
H(2B)	0.999 6 (17)	0.619 5 (23)	0.440 0 (16)
H(3B)	0.861 7 (15)	0.465 7 (22)	0.463 2 (14)
H(4B)	0.684 1 (13)	0.480 4 (20)	0.452 8 (13)
H(5B)	0.564 4 (15)	0.590 3 (21)	0.486 8 (15)
H(6B)	0.535 9 (19)	0.790 5 (25)	0.445 6 (18)
H(7B)	0.608 5 (19)	0.907 1 (28)	0.355 6 (18)
H(8B)	0.759 7 (17)	0.908 3 (27)	0.336 7 (17)

[a] Esd's, shown in parentheses, are right-adjusted to the least significant digit of the preceding number. They are derived from the inverse of the final least-squares matrix.

Table IV. Anisotropic Thermal Parameters[a,b] for $[(C_{10}H_8)Mn(CO)_3]_2$

Atom	U_{11}, Å^2	U_{22}, Å^2	U_{33}, Å^2	U_{12}, Å^2	U_{13}, Å^2	U_{23}, Å^2
Mn(1)	0.0400 (2)	0.0493 (2)	0.0327 (2)	−0.0028 (2)	0.0025 (2)	−0.0112 (2)
Mn(2)	0.0375 (2)	0.0431 (2)	0.0361 (2)	−0.0007 (2)	0.0003 (2)	−0.0093 (2)
C(11)	0.046 (2)	0.085 (2)	0.043 (2)	−0.003 (1)	0.002 (1)	−0.017 (1)
O(11)	0.069 (1)	0.159 (2)	0.052 (1)	−0.001 (1)	0.021 (1)	−0.021 (1)
C(12)	0.054 (2)	0.060 (2)	0.039 (1)	−0.011 (1)	−0.001 (1)	−0.014 (1)
O(12)	0.068 (1)	0.084 (2)	0.070 (1)	0.003 (1)	−0.021 (1)	−0.001 (1)
C(13)	0.066 (2)	0.071 (2)	0.047 (2)	−0.007 (2)	0.006 (1)	−0.017 (2)
O(13)	0.120 (2)	0.074 (2)	0.095 (2)	−0.039 (2)	0.010 (1)	−0.030 (1)
C(21)	0.054 (2)	0.060 (2)	0.050 (2)	−0.001 (1)	−0.002 (1)	−0.009 (2)
O(21)	0.097 (2)	0.092 (2)	0.062 (1)	0.006 (1)	−0.013 (1)	0.020 (1)
C(22)	0.053 (2)	0.056 (2)	0.040 (1)	−0.004 (1)	−0.005 (1)	−0.014 (1)
O(22)	0.063 (1)	0.094 (2)	0.063 (1)	0.003 (1)	0.018 (1)	−0.031 (1)
C(23)	0.052 (2)	0.063 (2)	0.052 (2)	−0.003 (2)	0.011 (1)	−0.015 (1)
O(23)	0.076 (1)	0.080 (1)	0.099 (2)	−0.031 (1)	0.013 (1)	−0.043 (1)
C(1A)	0.057 (2)	0.055 (2)	0.047 (2)	0.017 (1)	−0.010 (1)	−0.010 (1)
C(2A)	0.037 (1)	0.084 (2)	0.047 (2)	−0.001 (1)	−0.001 (1)	−0.021 (1)
C(3A)	0.047 (1)	0.054 (2)	0.033 (1)	−0.011 (1)	0.004 (1)	−0.012 (1)
C(4A)	0.041 (1)	0.038 (1)	0.030 (1)	−0.001 (1)	0.002 (1)	0.002 (1)
C(5A)	0.040 (1)	0.057 (2)	0.041 (1)	0.001 (1)	−0.002 (1)	−0.007 (1)
C(6A)	0.042 (1)	0.077 (2)	0.048 (2)	−0.013 (2)	0.007 (1)	−0.011 (2)
C(7A)	0.071 (2)	0.059 (2)	0.046 (2)	−0.026 (2)	0.013 (1)	−0.003 (1)
C(8A)	0.081 (2)	0.038 (1)	0.040 (1)	−0.005 (1)	0.002 (1)	0.002 (1)
C(9A)	0.052 (2)	0.042 (2)	0.030 (1)	−0.001 (1)	−0.002 (1)	−0.005 (1)
C(10A)	0.039 (1)	0.042 (1)	0.023 (1)	−0.003 (1)	−0.001 (1)	−0.008 (1)
C(1B)	0.054 (2)	0.069 (2)	0.045 (2)	−0.020 (2)	0.014 (1)	−0.009 (1)
C(2B)	0.038 (1)	0.078 (2)	0.053 (2)	0.006 (2)	0.003 (1)	−0.023 (2)
C(3B)	0.052 (2)	0.044 (2)	0.044 (1)	0.012 (1)	−0.006 (1)	−0.013 (1)
C(4B)	0.043 (1)	0.037 (1)	0.029 (1)	−0.003 (1)	0.004 (1)	0.001 (1)
C(5B)	0.042 (1)	0.070 (2)	0.045 (2)	−0.006 (1)	0.009 (1)	−0.020 (1)
C(6B)	0.044 (2)	0.073 (2)	0.075 (2)	0.017 (2)	−0.005 (1)	−0.029 (2)
C(7B)	0.076 (2)	0.049 (2)	0.070 (2)	0.024 (2)	−0.023 (2)	−0.007 (2)
C(8B)	0.082 (2)	0.038 (2)	0.053 (2)	−0.000 (1)	−0.007 (2)	0.007 (1)
C(9B)	0.048 (1)	0.041 (1)	0.033 (1)	−0.003 (1)	0.004 (1)	−0.003 (1)
C(10B)	0.037 (1)	0.037 (1)	0.029 (1)	0.003 (1)	−0.000 (1)	−0.006 (1)

Atom	U, Å^2	Atom	U, Å^2	Atom	U, Å^2
H(1A)	0.051 (7)	H(2A)	0.056 (7)	H(3A)	0.048 (7)
H(4A)	0.026 (5)	H(5A)	0.041 (10)	H(6A)	0.052 (7)
H(7A)	0.064 (8)	H(8A)	0.053 (7)	H(1B)	0.069 (8)
H(2B)	0.059 (7)	H(3B)	0.044 (7)	H(4B)	0.030 (5)
H(5B)	0.047 (7)	H(6B)	0.075 (9)	H(7B)	0.081 (9)
H(8B)	0.067 (8)				

[a] The anisotropic thermal parameter is defined by the following expression: $\exp[-2\pi^2(U_{11}h^2a^{*2} + U_{22}k^2b^{*2} + U_{33}l^2c^{*2} + 2U_{12}hka^*b^* + 2U_{13}hla^*c^* + 2U_{23}klb^*c^*)]$. [b] Isotropic thermal parameters are given for hydrogen atoms.

on the CDC 6400 computer at the State University of New York at Buffalo.

Scattering factors for neutral manganese, carbon, and oxygen were taken from the compilation of Cromer and Waber;[16] for hydrogen, the "best floated spherical H atom" values of Stewart et al.[17] were used. Both the real ($\Delta f'$) and imaginary ($\Delta f''$) components of anomalous dispersion were included for all nonhydrogen atoms, using the values of Cromer and Liberman.[18]

The function minimized during least-squares refinement was $\sum w(|F_o| - |F_c|)^2$, where $w = [\sigma(|F_o|)]^{-2}$. Discrepancy indices used in the text are defined in eq 1 and 2. The "goodness of fit" (GOF)

$$R_F\,(\%) = \left[\frac{\Sigma||F_o| - |F_c||}{\Sigma|F_o|}\right] \times 100 \qquad (1)$$

$$R_{wF}\,(\%) = \left[\frac{\Sigma w(|F_o| - |F_c|)^2}{\Sigma w|F_o|^2}\right]^{1/2} \times 100 \qquad (2)$$

is defined by eq 3, wherein NO is the number of observations and

$$\mathrm{GOF} = \left[\frac{\Sigma w(|F_o| - |F_c|)^2}{(\mathrm{NO} - \mathrm{NV})}\right]^{1/2} \qquad (3)$$

NV is the number of variables.

The structure was solved by symbolic addition. Normalized structure factor amplitudes, $|E(hkl)|$, were generated from $|F_o(hkl)|$ values using eq 4. Here the summation is over all N atoms in the unit cell, $\langle|E(hkl)|^2\rangle$ is normalized by a scale factor, $f[j, \theta(hkl)]$ is the scattering factor for the jth atom at the Bragg angle $\theta(hkl)$, and

$$|E(hkl)| = |F_o(hkl)|\left[\epsilon \sum_{j=1}^{j=N} f^2[j, \theta(hkl)]\right]^{-1/2} \qquad (4)$$

ϵ is a coefficient which corrects for the effects of space group symmetry. The statistical distribution of $|E|$ values was in keeping with that expected for a centrosymmetric crystal (see Table II).

The $|E|$ values were tested for large Σ_2 interactions by FAME. The origin of the unit cell was defined by assigning positive phases to three strong reflections of appropriate parity (067, $|E| = 3.05$; 31$\bar{8}$, $|E| = 2.92$; 322, $|E| = 2.82$). Three additional strong reflections of differing parity and many Σ_2 interactions (224, $|E| = 2.78$; 55$\bar{7}$, $|E| = 2.74$; 563, $|E| = 2.67$) were assigned symbols. Application of the symbolic addition procedure by MAGIC generated symbolic signs for 470 reflections with $|E| > 1.5$. Assignments of real signs (+ or −) to symbols provided eight solutions. That of the second lowest "contradiction index" yielded a chemically sensible "E map" from which the positions of the two independent manganese atoms could be quickly ascertained. Two cycles of full-matrix least-squares refinement of positional and isotropic thermal parameters of the manganese atoms led to $R_F = 47.8\%$ and $R_{wF} = 51.2\%$. A Fourier synthesis then led to the unambiguous location of all 32 remaining nonhydrogen atoms.

The analysis was continued using only the 1990 reflections of highest $|F_o|$ value. Refinement of positional and anisotropic thermal parameters for all nonhydrogen atoms, with hydrogen atoms included in calculated positions, led to convergence with $R_F = 2.21\%$, $R_{wF} = 2.86\%$, and GOF = 1.478.

At this point we returned to the full set of 2946 data and calculated a difference-Fourier map based upon the phasing of all nonhydrogen atoms ($R_F = 6.03\%$, $R_{wF} = 7.50\%$). The highest 16 peaks on this

Table V. Interatomic Distances and Esd's for $[(C_{10}H_8)Mn(CO)_3]_2$ (Å)

(a) Distances from Manganese Atom			
Mn(1)-C(11)	1.7813 (25)	Mn(2)-C(21)	1.7816 (26)
Mn(1)-C(12)	1.7988 (26)	Mn(2)-C(22)	1.7993 (25)
Mn(1)-C(13)	1.7996 (30)	Mn(2)-C(23)	1.7979 (27)
Mn(1)-C(1A)	2.1449 (27)	Mn(2)-C(1B)	2.1439 (26)
Mn(1)-C(2A)	2.1269 (26)	Mn(2)-C(2B)	2.1282 (27)
Mn(1)-C(3A)	2.1305 (26)	Mn(2)-C(3B)	2.1288 (26)
Mn(1)-C(10A)	2.1611 (21)	Mn(2)-C(10B)	2.1722 (21)
Mn(1)-C(9A)	2.1781 (22)	Mn(2)-C(9B)	2.1910 (23)
(b) Carbonyl Bond Lengths			
C(11)-O(11)	1.1487 (32)	C(21)-O(21)	1.1538 (34)
C(12)-O(12)	1.1477 (32)	C(22)-O(22)	1.1486 (31)
C(13)-O(13)	1.1436 (38)	C(23)-O(23)	1.1475 (34)
(c) Distances within Diazulene Ligand			
C(1A)-C(2A)	1.399 (4)	C(1B)-C(2B)	1.394 (4)
C(2A)-C(3A)	1.411 (4)	C(2B)-C(3B)	1.406 (4)
C(3A)-C(10A)	1.422 (3)	C(3B)-C(10B)	1.409 (3)
C(10A)-C(9A)	1.422 (3)	C(10B)-C(9B)	1.434 (3)
C(9A)-C(1A)	1.432 (4)	C(9B)-C(1B)	1.425 (4)
C(10A)-C(4A)	1.499 (3)	C(10B)-C(4B)	1.495 (3)
C(4A)-C(5A)	1.505 (3)	C(4B)-C(5B)	1.495 (4)
C(5A)-C(6A)	1.316 (4)	C(5B)-C(6B)	1.319 (4)
C(6A)-C(7A)	1.442 (4)	C(6B)-C(7B)	1.440 (4)
C(7A)-C(8A)	1.331 (4)	C(7B)-C(8B)	1.322 (5)
C(8A)-C(9A)	1.455 (4)	C(8B)-C(9B)	1.455 (4)
C(4A)-C(4B)	1.580 (3)		
(d) Carbon-Hydrogen Distances			
C(1A)-H(1A)	0.940 (24)	C(1B)-H(1B)	0.909 (27)
C(2A)-H(2A)	0.960 (25)	C(2B)-H(2B)	0.970 (25)
C(3A)-H(3A)	0.968 (24)	C(3B)-H(3B)	0.930 (23)
C(4A)-H(4A)	0.938 (20)	C(4B)-H(4B)	0.921 (20)
C(5A)-H(5A)	0.951 (22)	C(5B)-H(5B)	0.960 (23)
C(6A)-H(6A)	0.942 (24)	C(6B)-H(6B)	0.891 (27)
C(7A)-H(7A)	0.978 (26)	C(7B)-H(7B)	0.870 (29)
C(8A)-H(8A)	0.967 (24)	C(8B)-H(8B)	0.935 (27)

map (peak heights 0.803 → 0.404 e Å^{-3}) were at the positions expected for the omitted hydrogen atoms. Hydrogen atoms were now included in their observed positions and their positional and isotropic thermal parameters were refined to convergence (R_F = 4.04%, R_{wF} = 3.26%) while all other parameters were held constant. Refinement of all parameters was now resumed. This was done in "blocks" due to core limitations of the computer. (1) All parameters for the first $C_{10}H_8Mn(CO)_3$ residue were refined along with the scale factor and parameters for the second Mn atom. (2) Parameters for the second $C_{10}H_8Mn(CO)_3$ residue were refined along with the scale factor and parameters for the first manganese atom. (3) Steps 1 and 2 were repeated until all shifts were less than 0.1σ. (4) Positional parameters for all 50 atoms were refined until all shifts were identically zero on the computer output (i.e., maximum shift $<5 \times 10^{-7}$). The final positional correlation matrix was used in ORFFE for calculating esd's on interatomic distances and angles. Final discrepancy indices were R_F = 3.98% and R_{wF} = 3.17% for all 2946 reflections; the "goodness of fit" was 1.084. The function $\sum w(|F_o| - |F_c|)^2$ showed no appreciable dependence either upon (sin θ)/λ or upon $|F_o|$; the weighting scheme is thus acceptable. There was no evidence for secondary extinction. The highest feature on a final difference-Fourier synthesis was a peak of height 0.36 e Å^{-3} at −0.167, 0.111, 0.500. The analysis is thus both correct and complete.

A table of observed and calculated structure factor amplitudes is available.[19] Positional parameters are collected in Table III; thermal parameters are listed in Table IV.

The Molecular Structure

Interatomic distances and their estimated standard deviations (esd's) are shown in Table V; bond angles and their esd's are given in Table VI. Least-squares planes are presented in Table VII.

Views of the $[(C_{10}H_8)Mn(CO)_3]_2$ molecule are shown in Figures 1 and 2. As can be seen from these figures, the molecule consists of two azulenetricarbonylmanganese fragments which are mutually linked by a carbon–carbon bond

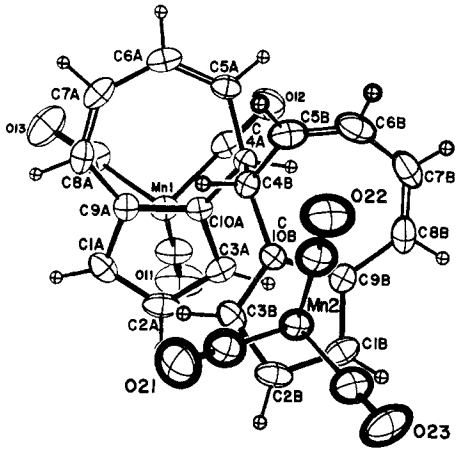

Figure 1. Stereochemistry and labeling of atoms in the $[(C_{10}H_8)Mn(CO)_3]_2$ molecule (ORTEP diagram; 30% ellipsoids for nonhydrogen atoms, with hydrogen atoms artificially represented as spheres of radius 0.10 Å).

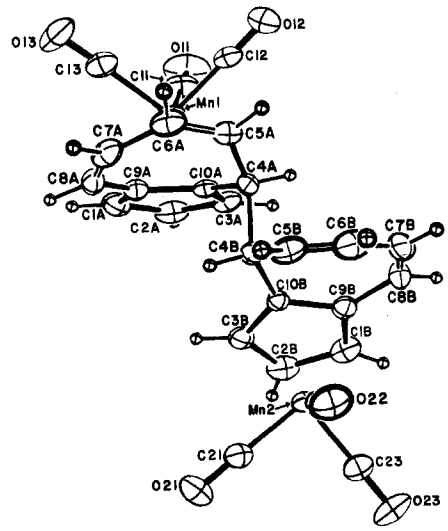

Figure 2. Another view of the $[(C_{10}H_8)Mn(CO)_3]_2$ molecule, showing the configuration of the 4,4′-diazulene ligand (ORTEP diagram).

[C(4A)–C(4B)]. The halves of the molecule are equivalent except for different rotameric orientations of the $Mn(CO)_3$ fragments bonded to the five-membered rings (cf. Figure 1). The 4,4′-diazulene ligand has C_2 symmetry within the limits of experimental error. Thus, within a given molecule, the absolute configurations of C(4A) and C(4B) are identical. Each molecule is chiral, but the crystal as a whole is an ordered racemate by virtue of crystallographic $\bar{1}$ and *c*-glide symmetry elements. It is worth noting that a crystallographic study on the related molecule $[(C_{10}H_8)Mo(CO)_3CH_3]_2$ showed it to possess a crystallographic center of symmetry;[4] i.e., this molecule is a meso compound, the absolute configuration at C(4B) being inverted relative to that at C(4A) (see III).

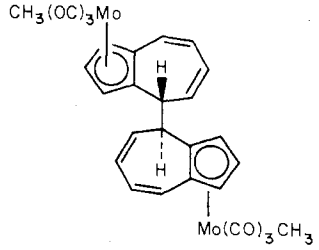

III

Table VI. Angles and Esd's within the $[(C_{10}H_8)Mn(CO)_3]_2$ Molecule (deg)

	(a) Angles around Manganese Atoms		
C(11)-Mn(1)-C(12)	91.75 (12)	C(21)-Mn(2)-C(22)	88.98 (12)
C(11)-Mn(1)-C(13)	93.01 (13)	C(21)-Mn(2)-C(23)	92.03 (12)
C(12)-Mn(1)-C(13)	93.13 (12)	C(22)-Mn(2)-C(23)	93.16 (12)
C(1A)-Mn(1)-C(2A)	38.22 (11)	C(1B)-Mn(2)-C(2B)	38.08 (11)
C(2A)-Mn(1)-C(3A)	38.72 (11)	C(2B)-Mn(2)-C(3B)	38.57 (10)
C(3A)-Mn(1)-C(10A)	38.69 (09)	C(3B)-Mn(2)-C(10B)	38.24 (09)
C(10A)-Mn(1)-C(9A)	38.27 (08)	C(10B)-Mn(2)-C(9B)	38.38 (08)
C(9A)-Mn(1)-C(1A)	38.67 (09)	C(9B)-Mn(2)-C(1B)	38.35 (09)
	(b) Angles within Carbonyl Groups		
Mn(1)-C(11)-O(11)	178.09 (23)	Mn(2)-C(21)-O(21)	179.58 (24)
Mn(1)-C(12)-O(12)	179.36 (24)	Mn(2)-C(22)-O(22)	176.88 (22)
Mn(1)-C(13)-O(13)	177.01 (25)	Mn(2)-C(23)-O(23)	178.65 (24)
	(c) C-C-C Angles within Five-Membered Rings		
C(9A)-C(1A)-C(2A)	108.41 (24)	C(9B)-C(1B)-C(2B)	109.51 (25)
C(1A)-C(2A)-C(3A)	108.70 (23)	C(1B)-C(2B)-C(3B)	107.19 (24)
C(2A)-C(3A)-C(10A)	107.76 (22)	C(2B)-C(3B)-C(10B)	109.69 (23)
C(3A)-C(10A)-C(9A)	108.16 (20)	C(3B)-C(10B)-C(9B)	106.95 (20)
C(10A)-C(9A)-C(1A)	106.97 (21)	C(10B)-C(9B)-C(1B)	106.66 (21)
	(d) C-C-C Angles within Seven-Membered Rings		
C(10A)-C(4A)-C(5A)	113.96 (20)	C(10B)-C(4B)-C(5B)	114.54 (20)
C(4A)-C(5A)-C(6A)	127.64 (24)	C(4B)-C(5B)-C(6B)	126.84 (24)
C(5A)-C(6A)-C(7A)	129.11 (26)	C(5B)-C(6B)-C(7B)	129.05 (27)
C(6A)-C(7A)-C(8A)	127.35 (26)	C(6B)-C(7B)-C(8B)	128.16 (28)
C(7A)-C(8A)-C(9A)	126.92 (25)	C(7B)-C(8B)-C(9B)	126.57 (26)
C(8A)-C(9A)-C(10A)	127.28 (21)	C(8B)-C(9B)-C(10B)	126.99 (22)
C(9A)-C(10A)-C(4A)	125.59 (19)	C(9B)-C(10B)-C(4B)	125.70 (20)
	(e) Exterior C-C-C Angles		
C(1A)-C(9A)-C(8A)	125.70 (23)	C(1B)-C(9B)-C(8B)	126.26 (24)
C(3A)-C(10A)-C(4A)	125.64 (21)	C(3B)-C(10B)-C(4B)	126.38 (21)
C(4B)-C(4A)-C(5A)	111.46 (18)	C(4A)-C(4B)-C(5B)	110.75 (19)
C(4B)-C(4A)-C(10A)	108.82 (18)	C(4A)-C(4B)-C(10B)	109.07 (18)
	(f) C-C(sp^2)-H Angles		
C(9A)-C(1A)-H(1A)	123.1 (14)	C(9B)-C(1B)-H(1B)	122.1 (17)
C(2A)-C(1A)-H(1A)	128.5 (14)	C(2B)-C(1B)-H(1B)	128.3 (17)
C(1A)-C(2A)-H(2A)	127.2 (15)	C(1B)-C(2B)-H(2B)	124.5 (14)
C(3A)-C(2A)-H(2A)	124.1 (15)	C(3B)-C(2B)-H(2B)	128.3 (14)
C(2A)-C(3A)-H(3A)	127.6 (13)	C(2B)-C(3B)-H(3B)	129.6 (14)
C(10A)-C(3A)-H(3A)	124.6 (13)	C(10B)-C(3B)-H(3B)	120.7 (14)
C(4A)-C(5A)-H(5A)	114.7 (13)	C(4B)-C(5B)-H(5B)	113.6 (14)
C(6A)-C(5A)-H(5A)	117.4 (13)	C(6B)-C(5B)-H(5B)	119.5 (14)
C(5A)-C(6A)-H(6A)	117.5 (15)	C(5B)-C(6B)-H(6B)	117.4 (17)
C(7A)-C(6A)-H(6A)	113.3 (15)	C(7B)-C(6B)-H(6B)	113.5 (17)
C(6A)-C(7A)-H(7A)	113.1 (15)	C(6B)-C(7B)-H(7B)	112.0 (19)
C(8A)-C(7A)-H(7A)	119.4 (15)	C(8B)-C(7B)-H(7B)	119.6 (19)
C(7A)-C(8A)-H(8A)	121.8 (14)	C(7B)-C(8B)-H(8B)	120.4 (16)
C(9A)-C(8A)-H(8A)	111.3 (14)	C(9B)-C(8B)-H(8B)	113.0 (16)
	(g) C-C(sp^3)-H Angles		
C(4B)-C(4A)-H(4A)	105.5 (12)	C(4A)-C(4B)-H(4B)	107.3 (12)
C(5A)-C(4A)-H(4A)	108.4 (11)	C(5B)-C(4B)-H(4B)	107.2 (12)
C(10A)-C(4A)-H(4A)	108.3 (11)	C(10B)-C(4B)-H(4B)	107.7 (12)

There are, then, three possible isomers of the 4,4′-diazulene ligand—a meso form of C_i symmetry (IV) and an enantiomeric pair (V and VI), each of C_2 symmetry. For any $[(C_{10}H_8)M(CO)_x]_2$ species, considerably more than three isomers are possible. There are three different isomers based upon IV, dependent upon whether the $M(CO)_x$ fragments lie above or below the five-membered rings. ("Above" and "below" can be defined relative to the C(4)–C(4′) bond—cf. Figure 2.) There are, similarly, three chiral isomers based upon V and three based upon VI (the latter forming enantiomeric pairs with those from V).

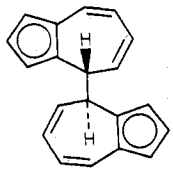

IV

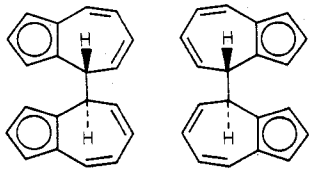

V VI

The observed isomers for $[(C_{10}H_8)Mn(CO)_3]_2$ (idealized C_2 symmetry, allowing for free rotation of the $Mn(CO)_3$ groups) and $[(C_{10}H_8)Mo(CO)_3CH_3]_2$ (C_i symmetry) each have the metal carbonyl fragments attached to the "outer" surfaces of the five-membered rings. This probably results from steric control of the synthetic reaction. However, it is still not clear why an enantiomeric pair of isomers (idealized C_2 symmetry) is obtained for $[(C_{10}H_8)Mn(CO)_3]_2$, while the meso form (C_i symmetry) is obtained for $[(C_{10}H_8)Mo(CO)_3CH_3]_2$. It may well be that the species isolated were simply those most easily extracted from solution and that both C_i and

Table VII. Least-Squares Planes[a,b] and Deviations of Atoms Therefrom[c]

Atom	Dev, Å	Atom	Dev, Å
Plane IA:	0.364 87X + 0.250 96Y + 0.896 60Z = 8.7554		
C(1A)*	−0.0037 (27)	H(1A)	−0.036 (23)
C(2A)*	+0.0041 (28)	H(2A)	+0.009 (24)
C(3A)*	−0.0028 (25)	H(3A)	+0.025 (23)
C(10A)*	+0.0005 (21)	C(4A)	+0.1845 (23)
C(9A)*	+0.0019 (22)	C(8A)	+0.0634 (27)
Mn(1)	−1.7778 (3)	C(5A)	−0.6462 (25)
C(11)	−2.7184 (27)	C(6A)	−0.7722 (28)
C(12)	−2.8043 (25)	C(7A)	−0.2636 (28)
C(13)	−2.7695 (28)		
Plane IB:	−0.073 66X + 0.304 42Y + 0.949 69Z = 7.1628		
C(1B)*	+0.0028 (28)	H(1B)	+0.046 (26)
C(2B)*	+0.0000 (28)	H(2B)	−0.023 (24)
C(3B)*	−0.0028 (26)	H(3B)	−0.034 (22)
C(10B)*	+0.0044 (21)	C(4B)	−0.2070 (23)
C(9B)*	−0.0044 (23)	C(8B)	−0.0844 (29)
Mn(2)	+1.7851 (3)	C(5B)	+0.5814 (27)
C(21)	+2.7604 (26)	C(6B)	+0.6784 (31)
C(22)	+2.8723 (25)	C(7B)	+0.1698 (31)
C(23)	+2.7485 (27)		
Plane IIA:	0.051 69X + 0.378 36Y + 0.924 21Z = 6.3346		
C(5A)*	+0.0381 (25)	H(5A)	−0.119 (21)
C(6A)*	−0.0818 (28)	H(6A)	−0.318 (23)
C(7A)*	+0.0804 (28)	H(7A)	+0.215 (25)
C(8A)*	−0.0367 (27)	H(8A)	+0.061 (23)
Plane IIB:	0.213 77X + 0.371 08Y + 0.903 66Z = 10.3187		
C(5B)*	−0.0410 (27)	H(5B)	+0.154 (22)
C(6B)*	+0.0891 (31)	H(6B)	+0.294 (27)
C(7B)*	−0.0884 (31)	H(7B)	−0.220 (28)
C(8B)*	+0.0403 (29)	H(8B)	−0.001 (26)

[a] Equations to planes are expressed in orthonormal coordinates (X, Y, Z) which are related to the fractional coordinates (x, y, z) via the transformation

$$\begin{pmatrix} X \\ Y \\ Z \end{pmatrix} = \begin{pmatrix} a & 0 & c\cos\beta \\ 0 & b & 0 \\ 0 & 0 & c\sin\beta \end{pmatrix} \begin{pmatrix} x \\ y \\ z \end{pmatrix}$$

[b] Only atoms marked with an asterisk were included in calculation of the plane. [c] Important interplanar angles: plane IA–plane IIA = 19.53°; plane IB–plane IIB = 17.17°.

C_2 isomers exist for each of the two stoichiometries. However, further work on this problem is still necessary.

Within the present $[(C_{10}H_8)Mn(CO)_3]_2$ molecule, each manganese atom achieves the expected noble gas configuration by linkages to three carbonyl ligands and to a five-membered ring of the 4,4′-diazulene ligand.

Each of the $Mn(CO)_3$ groups deviates slightly, but significantly, from C_{3v} symmetry. Thus, Mn(1)–C(11) = 1.7813 (25) Å vs. Mn(1)–C(12) = 1.7988 (26) Å and Mn(1)–C(13) = 1.7996 (30) Å; similarly, Mn(2)–C(21) = 1.7816 (26) Å vs. Mn(2)–C(22) = 1.7993 (25) Å and Mn(2)–C(23) = 1.7979 (27) Å. Bond angles are also inequivalent with C(11)–Mn(1)–C(12) and C(21)–Mn(2)–C(22) having values of 91.75 (12) and 88.98 (12)° and being approximately 1.3 and 3.5° (respectively) more acute than the two remaining OC–Mn–CO angles in each system. However, the variations in bond distances and bond angles are not consistent with any simple electronic perturbation (bond distances suggest that atoms C(11) and C(21) are uniquely disposed within their $Mn(CO)_3$ groups; the data on bond angles suggest that C(13) and C(23) are uniquely positioned). These distortions are, presumably, the net result of intramolecular strain and intra- and intermolecular nonbonded repulsions.

Carbon–oxygen distances range from 1.1436 (38) to 1.1538 (34) Å, averaging 1.1483 Å. The Mn–C–O systems are all close to linear, the greatest distortions being for Mn(1)–C(13)–O(13) [177.01 (25)°] and Mn(2)–C(22)–O(22) [176.88 (22)°].

Distances of the manganese atoms from the carbon atoms of their associated five-membered rings vary significantly around the ring, but the pattern is consistent from one $(C_{10}H_8)Mn(CO)_3$ residue to the other; thus, in order of increasing distance: Mn(1)–C(2A) = 2.1269 (26) Å and Mn(2)–C(2B) = 2.1282 (27) Å; Mn(1)–C(3A) = 2.1305 (26) Å and Mn(2)–C(3B) = 2.1288 (26) Å; Mn(1)–C(1A) = 2.1449 (27) Å and Mn(2)–C(1B) = 2.1439 (26) Å; Mn(1)–C(10A) = 2.1661 (21) Å and Mn(2)–C(10B) = 2.1722 (21) Å; Mn(1)–C(9A) = 2.1781 (22) Å and Mn(1)–C(9B) = 2.1910 (23) Å. Nevertheless, the five-membered rings are planar within the limits of experimental error (root-mean-square deviations from planarity are 0.0032 Å for plane IA and 0.0037 Å for plane IB—see Table VII).

Individual bond lengths within the five-membered rings range 1.399 (4)–1.432 (4) Å in ring A and 1.394 (4)–1.434 (3) Å in ring B, the average value being 1.415 Å. The C–C–C bond angles range from 106.97 (21) to 108.70 (23)° in ring A and from 106.66 (21) to 109.69 (23)° in ring B, averaging 108.00° for each system (as expected for a planar pentagon). Atoms bonded to those of the five-membered rings are, on the average, displaced away from the manganese atoms. Thus, deviations of atoms from plane IA are −0.036 Å for H(1A), +0.009 Å for H(2A), +0.025 Å for H(3A), +0.185 Å for C(4A) and +0.063 Å for C(8A) [vs. −1.778 Å for Mn(1)]; similarly, deviations from plane IB are +0.046 Å for H(1B), −0.023 Å for H(2B), −0.034 Å for H(3B), −0.207 Å for C(4B) and −0.084 Å for C(8B) [vs. +1.785 Å for Mn(2)].

The seven-membered rings are markedly nonplanar, owing primarily to the tetrahedral geometry at C(4A) and C(4B). Deviations of carbon atoms of the seven-membered rings from the least-squares planes through the appropriate five-membered ring range from +0.185 to −0.772 Å in the "A" system and from −0.207 Å to +0.678 Å in the "B" system (see Table VII). It should be noted, also, that neither of the two *cis*-diene systems is planar (see planes IIA and IIB in Table VII). Bond distances within the seven-membered ring are both internally consistent and in agreement with accepted values. Thus $C(sp^3)$–$C(sp^2)$ single bonds [C(4A)–C(10A) = 1.499 (3) Å, C(4A)–C(5A) = 1.505 (3) Å, C(4B)–C(10B) = 1.495 (3) Å and C(4B)–C(5B) = 1.495 (4) Å] are in excellent agreement with the accepted value of 1.510 ± 0.005 Å.[20] Bond lengths with the two free *cis*-diene systems [C(5A)–C(6A) = 1.316 (4) Å, C(6A)–C(7A) = 1.442 (4) Å, C(7A)–C(8A) = 1.331 (4) Å; C(5B)–C(6B) = 1.319 (4) Å, C(6B)–C(7B) = 1.440 (4) Å, C(7B)–C(8B) = 1.322 (5) Å; average C=C = 1.322 Å, average C–C = 1.441 Å] may be compared with distances of 1.344 (14), 1.441 (15), and 1.352 (15) Å for the *cis*-diene systems in $[(C_{10}H_8)Mo(CO)_3CH_3]_2$[4] and 1.337 (5) Å, 1.483 (10), and 1.337 (5) Å in *trans*-buta-1,3-diene.[21] The bonds C(8A)–C(9A) and C(8B)–C(9B) have lengths of 1.455 (4) and 1.455 (4) Å, consistent with the accepted $C(sp^2)$–$C(sp^2)$ single-bond distance of 1.465 ± 0.005 Å.[20]

All angles within the seven-membered rings are uniformly larger than the appropriate ideal sp^2 or sp^3 value. Thus, the angles C(10A)–C(4A)–C(5A) and C(10B)–C(4B)–C(5B) have values of 113.96 (20) and 114.54 (20)° (respectively)—some 4.5–5.0° greater than the ideal tetrahedral angle of 109.47°. Other internal angles at sp^2-hybridized carbon atoms range from 125.59 (19) to 129.11 (26)° in the A ring and from 125.70 (20) to 129.05 (27)° within the B ring, as opposed to the ideal trigonal angle of 120.00°. These systematic increases must be related simply to ring size—the average internal angle for a planar heptagon is required to be 128.57° ($5\pi/7$ rad).

The C(4A)–C(4B) bond, which links the two azulene systems, has a length of 1.580 (3) Å—some 0.043 Å greater than the accepted $C(sp^3)$–$C(sp^3)$ distance of 1.537 ± 0.005

Å but completely consistent with bridging C–C bonds found in other species, viz., 1.561 (18) Å in $[(C_{10}H_8)Mo(CO)_3C-H_3]_2$[4], 1.585 (15) Å in $(C_{10}H_8)_2Fe$[7], 1.567 (12) Å in $(C_{10}-H_8)_2Fe_4(CO)_{10}$[6], 1.568 (7) Å in (pentalenyl)$_2$Fe,[22] and 1.584 (14) Å in 1,1′-tetramethylethyleneferrocene.[23]

Finally, we note that all hydrogen atoms have been located with reasonable precision. Individual C–H distances thus obtained range from 0.870 (29) to 0.978 (26) Å, averaging 0.939 Å. This is in good agreement with the value of 0.95 Å suggested by Churchill[24] as the optimum C–H distance for an x-ray crystallographic study.

Acknowledgment. This work was generously supported by the National Science Foundation through Grant CHE76-05564 (to M.R.C.). Time on a CDC 6400 computer was provided by the Computer Center of the State University of New York at Buffalo.

Registry No. $[(C_{10}H_8)Mn(CO)_3]_2$, 60965-83-5.

Supplementary Material Available: Listing of structure factor amplitudes (18 pages). Ordering information is given on any current masthead page.

References and Notes

(1) M. R. Churchill, *Inorg. Chem.*, **6**, 190 (1967).
(2) M. R. Churchill and P. H. Bird, *Chem. Commun.*, 746 (1967).
(3) M. R. Churchill and P. H. Bird, *Inorg. Chem.*, **7**, 1545 (1968).
(4) P. H. Bird and M. R. Churchill, *Inorg. Chem.*, **7**, 349 (1968).
(5) M. R. Churchill and P. H. Bird, *Inorg. Chem.*, **7**, 1793 (1968).
(6) M. R. Churchill and P. H. Bird, *Inorg. Chem.*, **8**, 1941 (1969).
(7) M. R. Churchill and J. Wormald, *Inorg. Chem.*, **8**, 716 (1969).
(8) M. R. Churchill, K. Gold, and P. H. Bird, *Inorg. Chem.*, **8**, 1956 (1969).
(9) M. R. Churchill and J. Wormald, *Inorg. Chem.*, **12**, 191 (1973).
(10) M. R. Churchill, *Prog. Inorg. Chem.*, **11**, 53 (1970); see, especially, pp 72–74.
(11) R. Burton, L. Pratt, and G. Wilkinson, *J. Chem. Soc.*, 4290 (1960).
(12) R. B. King and M. N. Ackermann, *Inorg. Chem.*, **13**, 637 (1974).
(13) Programs used for centering of reflections, autoindexing, refinement of cell parameters, axial photographs, and data collection are those described in "Syntex $P2_1$ Operations Manual", R. A. Sparks, Ed., Syntex Analytical Instruments, Cupertino, Calif., 1973.
(14) J. A. Ibers and W. C. Hamilton, Ed., "International Tables for X-Ray Crystallography", Vol. IV, Kynoch Press, Birmingham, England, 1974, Table 1.1A, p 8.
(15) U. W. Arndt and B. T. M. Willis, "Single Crystal Diffractometry", Cambridge University Press, Cambridge, England, 1966, pp 286–287.
(16) D. T. Cromer and J. T. Waber, *Acta Crystallogr.*, **18**, 104 (1965).
(17) R. F. Stewart, E. R. Davidson, and W. T. Simpson, *J. Chem. Phys.*, **42**, 3175 (1965).
(18) D. T. Cromer and D. Liberman, *J. Chem. Phys.*, **53**, 1891 (1970).
(19) Supplementary material.
(20) *Chem. Soc., Spec. Publ.*, **No. 18**, S15s (1965).
(21) A. Almenningen, O. Bastiansen, and M. Traettenberg, *Acta Chem. Scand.*, **12**, 1221 (1958).
(22) M. R. Churchill and K.-K. G. Lin, *Inorg. Chem.*, **12**, 2274 (1973).
(23) M. B. Laing and K. N. Trueblood, *Acta Crystallogr.*, **19**, 373 (1965).
(24) M. R. Churchill, *Inorg. Chem.*, **12**, 1213 (1973).

Contribution from the Department of Chemistry,
Wayne State University, Detroit, Michigan 48202

Cobalt(II)-Mediated Oxygenation of a Macrocyclic Ligand. X-Ray Structures of the Cobalt(II) and Cobalt(III) Products[1]

BILL DURHAM, THOMAS J. ANDERSON, JAY A. SWITZER, JOHN F. ENDICOTT,* and MILTON D. GLICK*

Received July 26, 1976 AIC60547W

Diaquo(5,7-dimethyl-1,4,8,11-tetraazacyclotetradeca-4,7-diene)cobalt(II) hexafluorophosphate, $[Co([14]4,7\text{-dieneN}_4)(OH_2)_2](PF_6)_2$, reacts with O_2 to form a new macrocyclic ligand ([14]4,7-dieneN$_4$-one) with a ketone oxygen on the central carbon of the 2,4-pentanediiminato moiety. The cobalt(II) center appears to be necessary for this reaction yet is not oxidized in the process. The crystal and molecular structures of $[Co([14]4,7\text{-dieneN}_4\text{-one})(OH_2)_2](ClO_4)_2$ and $[Co([14]4,7\text{-dieneN}_4\text{-one})Cl_2]ClO_4$ have been determined from three-dimensional x-ray data collected on an automatic diffractometer using Mo Kα radiation. The crystals of $[Co([14]4,7\text{-dieneN}_4\text{-one})(OH_2)_2](ClO_4)_2$ belong to the space group $P2_1/c$ with $a = 10.371$ (2) Å, $b = 15.055$ (3) Å, $c = 14.467$ (3) Å, $\beta = 106.39$ (2)°, and $Z = 4$. The crystals of $[Co([14]4,7\text{-dieneN}_4\text{-one})Cl_2]ClO_4$ belong to the space group $Pbca$ with $a = 12.030$ (2) Å, $b = 12.995$ (2) Å, $c = 23.523$ (4) Å, and $Z = 8$. Full-matrix least-squares refinement yielded conventional discrepancy factors of 0.062 for 1835 observed counter data and 0.038 for 1894 observed counter data, respectively. The ketone oxygen in both complexes is bent up from the plane of the two imine bonds.

Introduction

Reactions of dioxygen with transition metal complexes are numerous and varied. Among the better characterized are dioxygen reactions which result in (1) oxidation only of the metal center,[2] (2) dehydrogenation of coordinated ligands,[3,4] or (3) formation of metal–dioxygen adducts.[5,6] While the present study was in progress, Weiss and Goedken[7] reported their discovery of a dioxygen–cobalt reaction in which a 2,4-pentanediiminato moiety of the coordination complex was converted into a β-diimine moiety with an α,β-unsaturated carbonyl; evidence for this reaction was based on infrared and proton magnetic resonance spectroscopy. We now find analogous behavior in the $Co^{II}([14]4,7\text{-dieneN}_4)$[8] complexes recently reported by Cummings and co-workers.[9] Moreover we have isolated and structurally characterized the coordination complex product containing the α,β-unsaturated carbonyl in the macrocyclic [14]4,7-dieneN$_4$-one ligand.

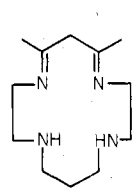

[14]4,7-dieneN$_4$

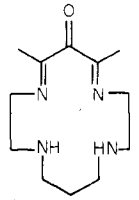

[14]4,7-dieneN$_4$-one

Experimental Section

A. Preparation of Complexes. 1. $[Co([14]4,7\text{-dieneN}_4\text{-one})Cl_2]ClO_4$.[8] A solution of $Co(O_2CCH_3)_2\cdot 4H_2O$ (14 g) in 500 ml of H_2O was prepared. A condenser was attached and the solution deaerated by bubbling deoxygenated N_2; then *N,N′*-bis(2-aminoethyl)-1,3-propanediamine (9.2 g) was deaerated and added by syringe to the preparative solution. After warming of this solution 11.6 g of deaerated 2,4-pentanedione was added. The mixture was refluxed